SUPPORTING INFORMATION

Title: A Silicon-Heteroaromatic System as Photosensitizer for Light-Driven Hydrogen Production by Hydrogenase Mimics
Author(s): Roman Goy, Ulf-Peter Apfel, Catherine Elleouet, Daniel Escudero, Martin Elstner, Helmar Görls, Jean Talarmin,* Philippe Schollhammer, Leticia González,* Wolfgang Weigand*

1   Electrochemical investigations
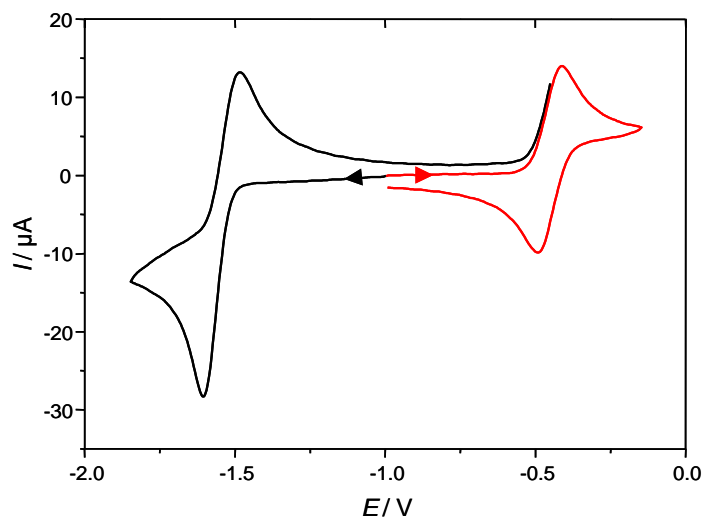
Figure S1: Cyclic voltammetry of **1**, (0.81 mM, black trace) and of [Fe$_2$(CO)$_4$(κ^2-I$_{Me}$-CH$_2$-I$_{Me}$)(μ-pdt)] (0.83 mM, red trace) in CH$_2$Cl$_2$-[NBu$_4$][PF$_6$] (vitreous carbon electrode, $v=0.2$ V s^{-1}; potentials are in V *vs.* Fc$^+$/Fc).
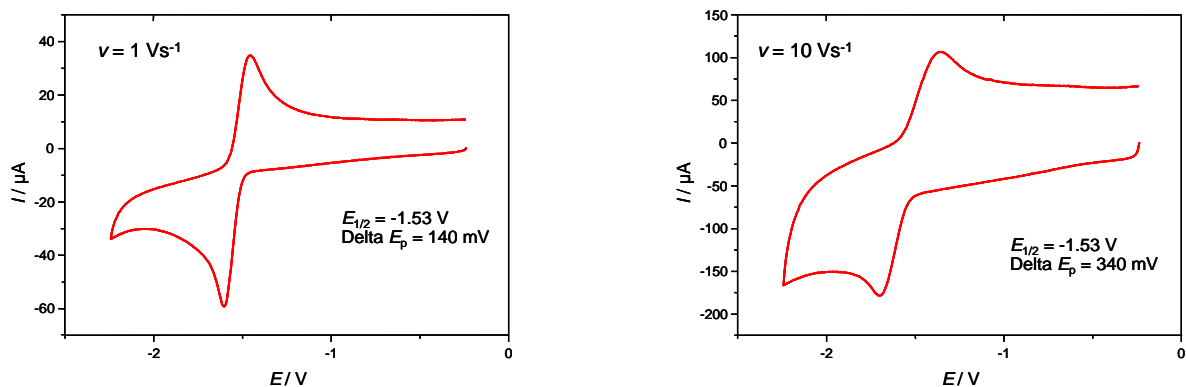

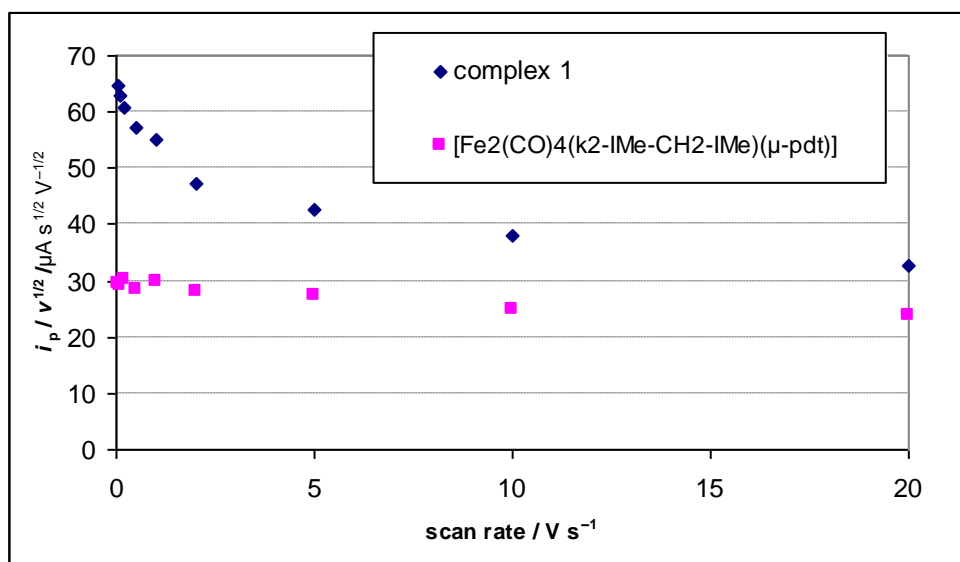**Figure S2**: Cyclic voltammetry of **1**, 0.4 mM in CH$_2$Cl$_2$-[NBu$_4$][PF$_6$] (vitreous carbon electrode, potentials are in V *vs.* Fc$^+$/Fc).

Figure S3: Scan rate dependence of the current for the reduction of **1** (0.81 mM, ◆) and for the oxidation of [Fe$_2$(CO)$_4$(κ^2-I$_{Me}$-CH$_2$-I$_{Me}$)(μ-pdt)] (0.83 mM, ■) in CH$_2$Cl$_2$-[NBu$_4$][PF$_6$] (vitreous carbon electrode).

2 Computational details

All calculations are based on density functional theory (DFT). Both geometry optimizations in the ground (S_0) and lowest triplet (T_1) excited states have been carried out with the hybrid functional B3LYP[1, 2] in combination with the 6-311G* basis set for all atoms. Relativistic effects were included in the Fe atoms using the MDF10 pseudopotential.[3] All the species have been characterized as true minima or transition states of the corresponding hyper-potential energy surfaces *via* a vibrational analysis. In Figure S4 the main geometrical features of complex **1** in its S_0 and T_1 optimized geometries are schematically shown. In Figure S5 and S6 the relevant orbitals involved in the relevant electronic excitations of **1** and **3** are depicted.

To reproduce the measured absorption UV-Vis spectrum, the lowest-lying 130 and 25 vertical singlet electronic excitation energies for **1** and **3**, respectively, were calculated using time-dependent DFT (TD-DFT) at the S_0 optimized geometry using the same functional and basis set employed in the geometry optimizations. Additionally, ΔSCF-DFT calculations have been performed to obtain the singlet-triplet splitting. Such calculations yield the adiabatic energy difference between the lowest triplet excited state and the ground state at their respective optimized geometries. The TD-DFT and ΔSCF-DFT calculations were performed in solution using heptane as solvent with the polarization continuum model.[4, 5] We point out here that the solvent employed in the experiments is hexane, which possesses very similar molecular properties as heptane. Therefore, we hardly expect any divergence in the results of our calculations performed in heptane. All the calculations were performed with the Gaussian03 program package.[6]
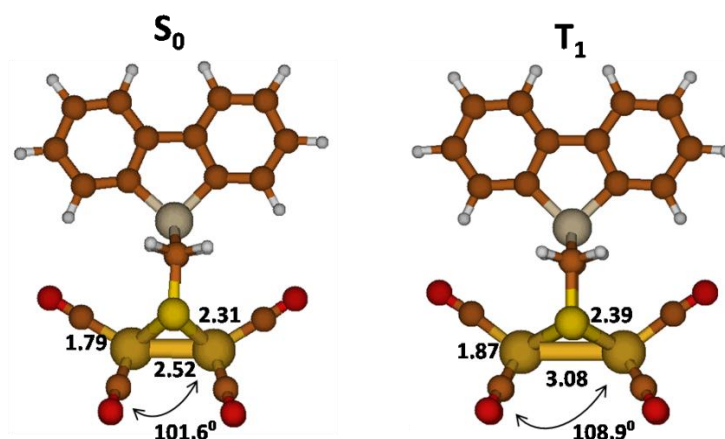

Figure S4. Relevant geometrical parameters of the optimized S_0 and T_1 geometries of complex **1**. Distances in Ångströms and angles in degrees.

L+3   **L+4**   **L+5**

L   **L+1**   **L+2**

H   **H-1**   **H-2**
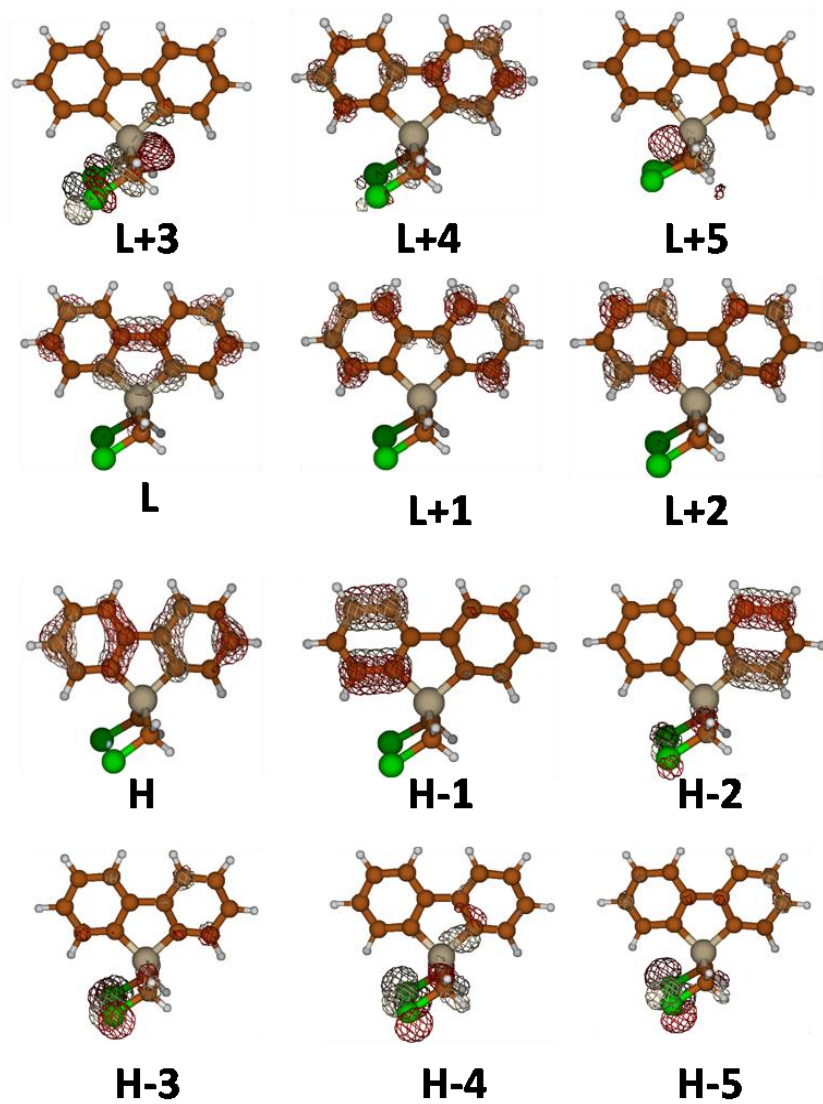
H-3   **H-4**   **H-5**

Figure S5. Relevant Kohn-Sham orbitals (B3LYP/6-311G*) for **3**.
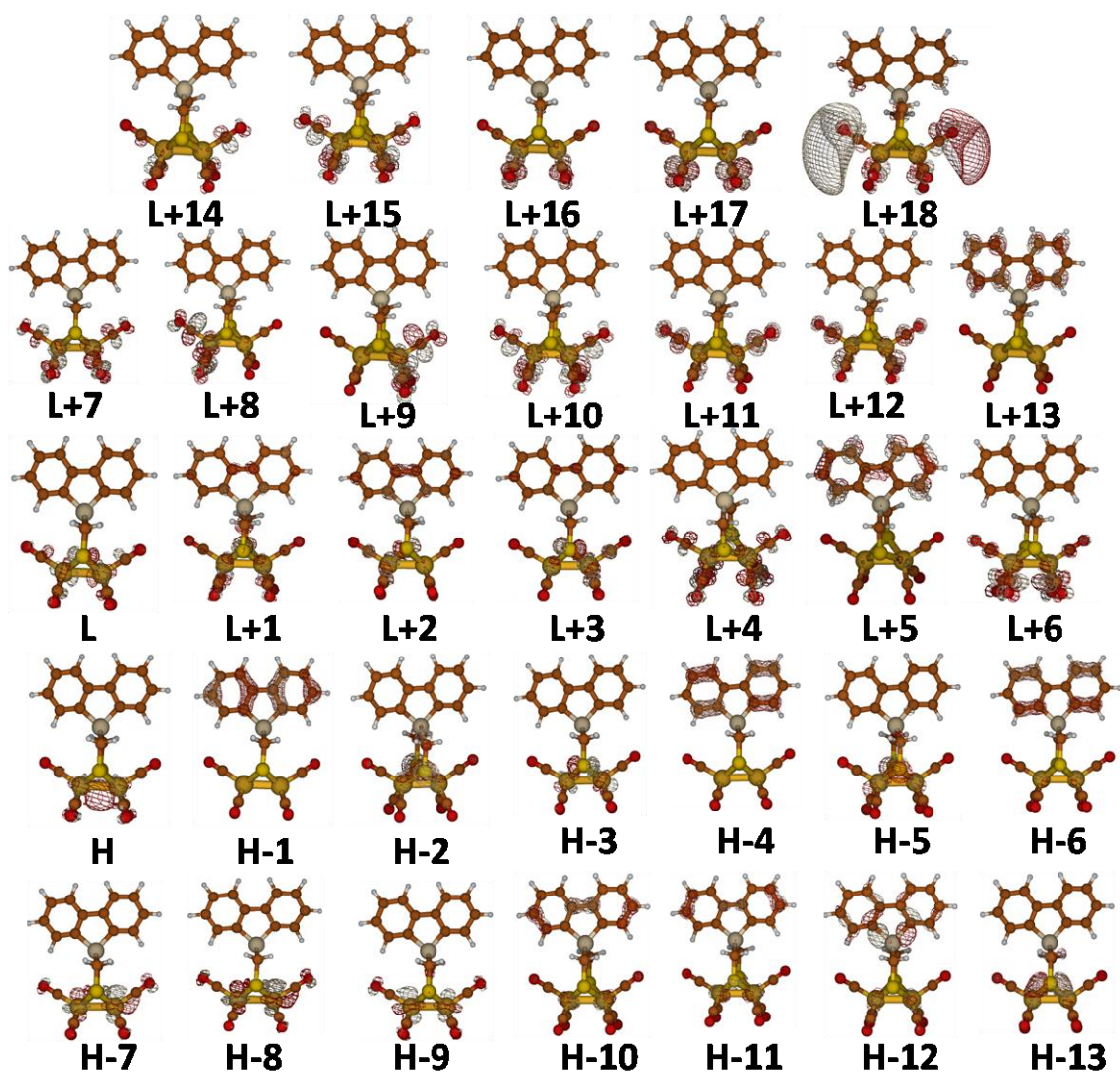
Figure S6. Relevant Kohn-Sham orbitals (B3LYP/6-311G*) for complex **1**.

3 TD-DFT results

Table S1. Main theoretical electronic singlet-singlet transition energies (ΔE) with corresponding oscillator strengths (f) and assignment for **1** and **3**. Number in parenthesis correspond to the wavefunction coefficient for the specified transition.

3

State	ΔE /nm	f	Assignment[a]
S_1	302	0.107	H→L (0.66) $\pi_{fl} \to \pi^*_{fl}$
S_2	274	0.130	H→L+1 (0.54) $\pi_{fl} \to \pi^*_{fl}$
S_4	240	0.440	H-1→L (0.46) $\pi_{fl} \to \pi^*_{fl}$
S_6	233	0.143	H-3→L (0.39) $n_{Cl} \to \pi^*_{fl}$ H→L+2 (-0.34) $\pi_{fl} \to \pi^*_{fl}$
S_9	221	0.045	H-1→L+1 (0.36) $\pi_{fl} \to \pi^*_{fl}$
S_{10}	219	0.195	H-2→L+1 (0.49) $\pi_{fl} \to \pi^*_{fl}$
S_{18}	202	0.100	H-3→L+1 (0.47) $n_{Cl} \to \pi^*_{fl}$

1

State	ΔE /nm	f	Assignment[b]
S_1	443	0.004	H-3→L (0.58) $3d_{Fe} \to \square^*_{Fe\text{-}Fe}$
S_4	398	0.104	H→L (0.60) $\square_{Fe\text{-}Fe} \to \square^*_{Fe\text{-}Fe}$
S_9	377	0.044	H-9→L (0.41) $3d_{Fe} \to \square^*_{Fe\text{-}Fe}$
S_{10}	359	0.015	H-5→L (0.39) $n_S \to \square^*_{Fe\text{-}Fe}$
S_{19}	315	0.036	H-1→L+1 (0.66) $\pi_{fl} \to 3d_{Fe} + \pi^*_{fl}$
S_{23}	297	0.015	H→L+8 (0.45) $\square_{Fe\text{-}Fe} \to \pi^*_{3\text{-}CO}$
S_{24}	295	0.019	H→L+9 (-0.45) $\square_{Fe\text{-}Fe} \to \pi^*_{3\text{-}CO}$
S_{26}	290	0.022	H→L+6 (0.49) $\square_{Fe\text{-}Fe} \to \pi^*_{6\text{-}CO}$
S_{27}	289	0.048	H-3→L+4 (0.33) $3d_{Fe} \to \pi^*_{6\text{-}CO}$
S_{28}	288	0.061	H-1→L+2 (0.66) $\pi_{fl} \to 3d_{Fe}$
S_{30}	282	0.017	H-1→L+3 (0.68) $\pi_{fl} \to 3d_{Fe} + n_S$
S_{32}	280	0.178	H-2→L+3 (0.68) $n_S \to 3d_{Fe} + n_S$
S_{33}	277	0.092	H-1→L+5 (0.68) $\pi_{fl} \to \pi^*_{fl}$
S_{46}	260	0.027	H-3→L+9 (0.29) $3d_{Fe} \to \pi^*_{3\text{-}CO}$
S_{48}	258	0.030	H-8→L+4 (0.31) $3d_{Fe} \to \pi^*_{6\text{-}CO}$
S_{55}	253	0.015	H-7→L+7 (0.31) $3d_{Fe} \to \pi^*_{3\text{-}CO}$
S_{56}	251	0.222	H-4→L+1 (0.53) $\pi_{fl} \to 3d_{Fe} + \pi^*_{fl}$
S_{58}	250	0.071	H→L+15 (0.25) $\square_{Fe\text{-}Fe} \to \pi^*_{6\text{-}CO}$
S_{60}	249	0.025	H-1→L+6 (0.31) $\pi_{fl} \to \pi^*_{6\text{-}CO}$
S_{61}	249	0.054	H-2→L+5 (0.43) $n_S \to \pi^*_{fl}$
S_{76}	241	0.025	H-3→L+7 (0.37) $3d_{Fe} \to \pi^*_{3\text{-}CO}$
S_{77}	239	0.071	H-4→L+2 (0.47) $\pi_{fl} \to 3d_{Fe}$
S_{78}	239	0.049	H-2→L+11 (0.40) $n_S \to \pi^*_{4\text{-}CO}$
S_{79}	237	0.071	H-4→L+3 (0.42) $\pi_{fl} \to 3d_{Fe} + n_S$
S_{84}	234	0.055	H-5→L+7 (0.48) $n_S \to \pi^*_{6\text{-}CO}$
S_{108}	223	0.094	H-4→L+5 (0.47) $\pi_{fl} \to \pi^*_{fl}$
S_{110}	223	0.157	H-6→L+5 (0.30) $\pi_{fl} \to \pi^*_{fl}$ H-6→L+3 (-0.31) $\pi_{fl} \to 3d_{Fe} + n_S$

S_{114}	222	0.037	H-5→L+10 (0.37) $n_S \rightarrow \pi^*_{6-CO}$
S_{115}	221	0.116	H-2→L+16 (0.34) $n_S \rightarrow \pi^*_{4-CO}$
S_{122}	218	0.020	H-8→L+7 (0.53) $3d_{Fe} \rightarrow \pi^*_{3-CO}$
S_{115}	217	0.026	H-2→L+18 (0.46) $n_S \rightarrow$ Rydberg

[a] The fl subindex denotes the 1-silafluorene moiety. [b] The 3-CO (4-CO, *etc*) subindex denotes a delocalized orbital among 3 (4, *etc*) of the CO ligands (see the involved orbitals in the excitations in Figure S6)

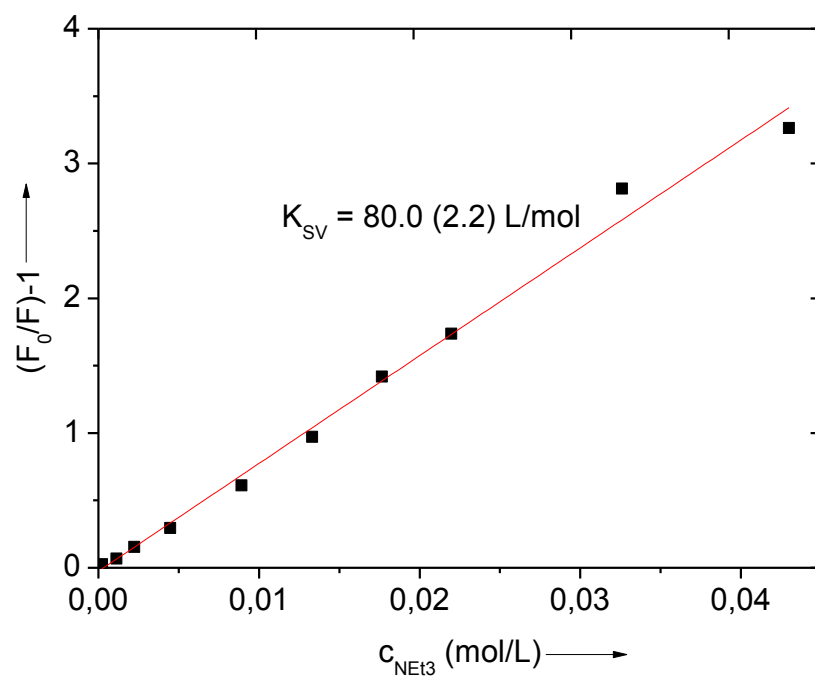## 4   Emission quenching of compound 3

Figure S7: Stern-Volmer plot for the emission quenching of compound **3** by triethylamine.
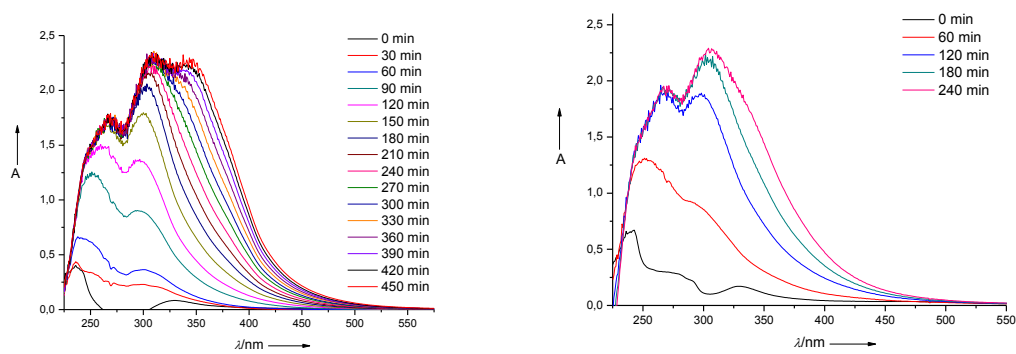
5   Irradiation of compound 1.

Figure S8: UV-vis spectra for compound **1** in acetonitrile (0.011 mM, left and 0.027 mM, right) and excitation at 254 nm.
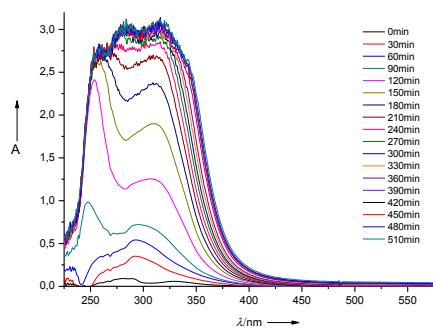

Figure S9: UV-vis spectra for compound **1** (0.011 mM) in the presence of trifluoroacetic acid (0.5 M) and triethylamine (0.5 M) in acetonitrile and excitation at 254 nm.

6 References

[1] A. D. Becke, *J. Chem. Phys.* **1993**, *98*, 5648–5652.

[2] C. T. Lee, W. T. Yang, R. G. Parr, *Phys. Rev. B.* **1988**, *37*, 785–789.

[3] a) M. Dolg, U. Wedig, H. Stoll, H. Preuss, *J. Chem. Phys.* **1987**, *86*, 866-872. b) B. Metz, H. Stoll, M. Dolg. *J. Chem. Phys.* **2000**, *113,* 2563-2569.

[4] M. Cossi, V. Barone, B. Menucci, J. Tomasi, *Chem. Phys. Lett.* **1998**, *286*, 253–260.

[5] B. Menucci, J. Tomasi, *J. Chem. Phys.* **1997**, 106, 5151–5158.

[6] Gaussian 03, Revision C.02, Frisch, M. J.; Trucks, G. W.; Schlegel, H. B.; Scuseria, G. E.; Robb, M. A.; Cheeseman, J. R.; Montgomery, Jr., J. A.; Vreven, T.; Kudin, K. N.; Burant, J. C.; Millam, J. M.; Iyengar, S. S.; Tomasi, J.; Barone, V.; Mennucci, B.; Cossi, M.; Scalmani, G.; Rega, N.; Petersson, G. A.; Nakatsuji, H.; Hada, M.; Ehara, M.; Toyota, K.; Fukuda, R.; Hasegawa, J.; Ishida, M.; Nakajima, T.; Honda, Y.; Kitao, O.; Nakai, H.; Klene, M.; Li, X.; Knox, J. E.; Hratchian, H. P.; Cross, J. B.; Bakken, V.; Adamo, C.; Jaramillo, J.; Gomperts, R.; Stratmann, R. E.; Yazyev, O.; Austin, A. J.; Cammi, R.; Pomelli, C.; Ochterski, J. W.; Ayala, P. Y.; Morokuma, K.; Voth, G. A.; Salvador, P.; Dannenberg, J. J.; Zakrzewski, V. G.; Dapprich, S.; Daniels, A. D.; Strain, M. C.; Farkas, O.; Malick, D. K.; Rabuck, A. D.; Raghavachari, K.; Foresman, J. B.; Ortiz, J. V.; Cui, Q.; Baboul, A. G.; Clifford, S.; Cioslowski, J.; Stefanov, B. B.; Liu, G.; Liashenko, A.; Piskorz, P.; Komaromi, I.; Martin, R. L.; Fox, D. J.; Keith, T.; Al-Laham, M. A.; Peng, C. Y.; Nanayakkara, A.; Challacombe, M.; Gill, P. M. W.; Johnson, B.; Chen, W.; Wong, M. W.; Gonzalez, C.; Pople, J. A.; Gaussian, Inc., Wallingford CT, **2004**.